SAND2013-5822C

Dispersion Engineering in Aluminum Nitride Phononic Crystal Plates

Bongsang Kim
Bosch Research and Technology Center
Palo Alto, CA, USA

Peter T. Rakich
Department of Applied Physics
Yale University
New Haven, CT, USA

Darren W. Branch, Peggy Clews, Janet Nguyen and Roy H. Olsson III
Sandia National Laboratories
Albuquerque, NM, USA
rholsso@sandia.gov

***Abstract*—The dispersive properties of phononic crystals can be utilized to manipulate the phononic impedance of a material and to engineer the frequency-delay response of time domain signal processing circuits. In this paper we study, in both the frequency and time domains, the dispersive properties of phononic crystals formed in thin suspended plates of aluminum nitride.**

Keywords-Aluminum nitride; dispersion; phononic crystal plates

I. INTRODUCTION

Recently, phononic crystals micromachined in thin suspended plates, with lateral and thickness dimensions on order of 100 nm to several microns, have been demonstrated for applications in RF signal processing [1-5] and thermal management [6]. Signal processing devices such as cavities and waveguides have been extensively studied and previously reported. In this paper we explore the dispersive properties of phononic crystals formed from etching a square lattice of circular air holes in a 750 nm thick, suspended aluminum nitride (AlN) membrane. The lattice constant is held constant at 5 μm, while the inclusion radius is varied from 0.5 to 1.75 μm. Ultra-wide bandwidth AlN piezoelectric transducers centered at 400 and 800 MHz are used to interrogate the responses of the phononic crystals. The dispersion of the phononic crystal plates is studied experimentally not only in the frequency domain, but also using time domain transmission and measurements. Deaf bands [4] in the phononic crystal frequency response are observed, which shift to lower frequencies as the hole radius is increased. A marked increase in the group delay is observed at the phononic crystal band-edge, coinciding with a flattening of the dispersion curve. Broad band pulses launched using the 400 and 800 MHz AlN transducers are utilized to characterize the phononic crystal time domain responses. Enlarging of the hole radius is shown to significantly increase the dispersion, as evidenced by an increase in both the absolute delay and width of the received pulses.

II. MOTIVATION

A. Low Impedance Phononic Media

The efficiency of photon-phonon coupling through optomechanical interactions, such as those reported in [7], depends on the magnitude of the optical forces generated and is inversely proportional to the mechanical impedance of the Brillouin active phonon modes

$$G_B \propto \frac{1}{Z(\Omega)}. \quad (1)$$

To date, virtually all optomechanical processes produce strong photon-phonon coupling by use of narrow-band impedance reductions associated with sharp phononic resonances [8]. We are investigating phononic crystals as a means of reducing the effective phononic impedance over much wider bandwidths than what can be achieved with high-Q cavities. This will enable efficient optomechanical coupling over the wide bandwidths needed for signal processing of modern communications waveforms.

B. Acoustic Signal Processing Circuits

Directly tailoring the dispersive properties of Lamb wave devices using phononic crystals offers the ability to construct passive time domain signal processing circuits, such as correlators and pulse compressors, with arbitrary delay versus frequency. Directly engineering the dispersion of the acoustic media, rather than achieving dispersion at the device level using frequency dependent mirrors or chirped interdigitated transducers [9], could offer lower loss as the parasitic capacitance of the transducers can be lower and energy is not inadvertently lost to the substrate.

III. DEVICE DESIGN AND FABRICATION

The fabrication process used to realize the phononic crystals studied in this work and the interrogating AlN transducers is shown in Figure 1. A) The fabrication begins with high resistivity six-inch Si wafers upon which a 0.6 μm oxide and a 2 μm polysilicon release layer are consecutively

This work was supported by the DDRE under Air Force contract number FA8721-05-C-000,the MesoDynamic Architectures program at DARPA under the direction of Dr. Jeffrey Rogers. Sandia National Laboratories is a multi-program laboratory managed and operated by Sandia Corporation, a wholly owned subsidiary of Lockheed Martin Corporation, for the U.S. Department of Energy's National Nuclear Security Administration under contract DE-AC04-94AL85000.

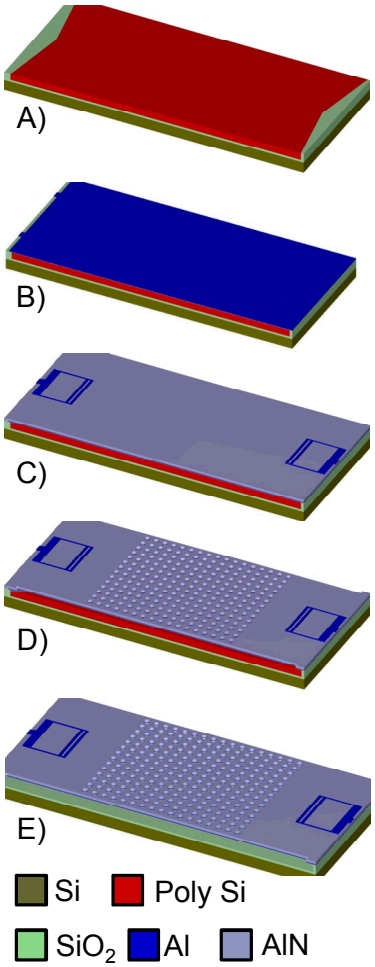

Figure 1. AlN phononic crystal fabrication process.

deposited. The polysilicon is then patterned to define where the AlN phononic crystal membranes will be undercut and suspended from the substrate. The taper seen in the polysilicon release layer at both ends of the device membrane is designed to prevent coherent reflections of the acoustic wave from the anchored boundary back into the phononic crystal test structure. Next, an oxide layer is deposited and chemically mechanically polished to expose the patterned polysilicon release layer. B) A thin, 100 nm, oxide layer is deposited and tungsten plugs (not shown) are machined into the oxide to make contact to the bottom electrode. Next, the electrically grounded bottom electrode, formed from 20/50/100 nm of Ti/TiN/Al is deposited and patterned. C) A 0.75 µm layer of AlN is sputter deposited and vias (not shown) in the AlN are etched landing on the tungsten plugs. A top electrode layer of 200/50 nm of Al/TiN is deposited and patterned to form the piezoelectric transducers. D) The phononic crystal air inclusions and release trenches are etched to expose the polysilicon release layer. E) The phononic crystal device is suspended from the substrate using a dry release in XeF_2.

A scanning electron microscope image (SEM) of an AlN phononic crystal device fabricated using the process in Figure 1, is shown in Figure 2. The device in Figure 2 has a 400 MHz

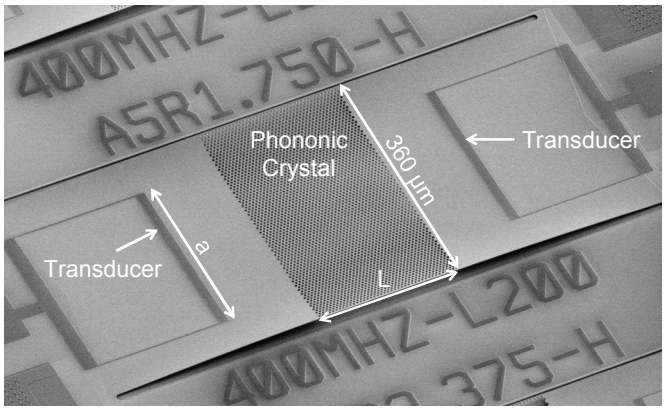

Figure 2. Scanning electron microscope image of an AlN phononic crystal.

AlN transducer designed to launch wide bandwidth S0 Lamb waves. The transducer is designed with a single, 12.5 µm wide electrode finger to achieve a very wide bandwidth. The electrode finger is designed to have a width of ½ of an acoustic wavelength (25 µm at 400 MHz), as opposed to a more standard ¼ acoustic wavelength (λ) design, to minimize reflections at the transducer interface. The transducer has an aperture, *a*, of 10 wavelengths, 250 µm, to come as closely as possible to launching a plane wave as the maximum release undercut in the fabrication process will allow. The transducers are spaced approximately 100 µm from the phononic crystals.

The 800 MHz S0 Lamb wave transducers, also utilized in this work, are schematically depicted in Figure 1 E). The 800 MHz transducers also have a finger width of λ/2 (6.25 µm), an aperture of 10λ (125 µm) and are spaced approximately 100 µm from the phononic crystals. The 800 MHz transducers, however, utilize two electrically connected half wavelength transducer fingers on a one wavelength pitch in order to achieve the same absolute bandwidth as the 400 MHz transducers. Table 1 summarizes the transducer designs.

The phononic crystal depicted in Figure 2 has a lattice constant, l_c, of 5 µm and an inclusion radius, *r*, of 1.75 µm. The length of the phononic crystal in Figure 2 is 200 µm and the width of both the phononic crystal and the membrane are 360 µm. The dimensions of the square lattice phononic crystals reported in this work are summarized in Table 2. While we studied phononic crystal lattices of 200, 300 and 400 µm in length, only the 400 µm lattices are reported as these had the largest impact on the overall device dispersion.

Table 1. Transducer Design Parameters

Frequency	# of Fingers	Electrode Width	Electrode Pitch	Aperture
400 MHz	1	λ/2 = 12.5 µm	N/A	10λ = 250 µm
800 MHz	2	λ/2 = 6.25 µm	λ = 12.5 µm	10λ = 125 µm

Table 2. Phononic Crystal Device Parameters and Average Measured Delay.

Device	Trans-ducer Design (MHz)	Inclusion Radius (µm)	Lattice Constant (µm)	Phononic Crystal Length (µm)	Average Measured Delay (ns)
Control A	400	N/A	N/A	N/A	61.6
Lattice1 A	400	0.5	5	400	62.9
Lattice2 A	400	1.25	5	400	70.6
Lattice3 A	400	1.75	5	400	81.8
Control B	800	N/A	N/A	N/A	61.7
Lattice1 B	800	0.5	5	400	63.9
Lattice2 B	800	1.25	5	400	79.8
Lattice3 B	800	1.75	5	400	99.9

IV. MEASUREMENTS

A. Frequency Domain Characterization

The devices in Table 2 were measured and the frequency responses characterized using a PNA E8358A network analyzer from Agilent Technologies. The measured frequency responses of the A devices with 400 MHz transducers are shown in Figure 3 with the responses of the B devices with 800 MHz transducers shown in Figure 4. While none of these lattices has air inclusions large enough to form a complete phononic bandgap, deaf bands [4] for the S0 Lamb waves are seen in the frequency responses, moving to lower frequencies as the size of the inclusions becomes larger.

The phononic crystal group delay is of particular relevance to the phononic crystal effective impedance and dispersion. For example, see Figure 5, which shows the correspondence of the transmission group delay of the phononic crystal with the phononic band diagram for Lattice3, with a lattice constant of 5 µm and an inclusion radius of 1.75 µm. The gray shaded region indicates the frequency range over which the phononic crystal prevents the propagation of S0 Lamb waves. At the band-edge (~480 MHz) a marked increase in group delay is observed, coinciding with a flattening of the dispersion curve. These data reveal that the transducer-to-transducer group delay

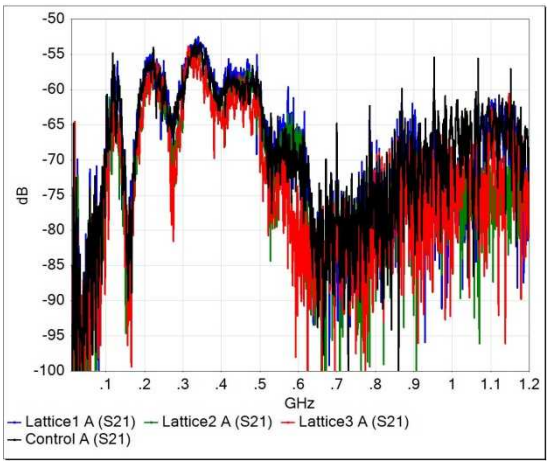

Figure 3. Frequency response for the A devices with 400 MHz transducers.

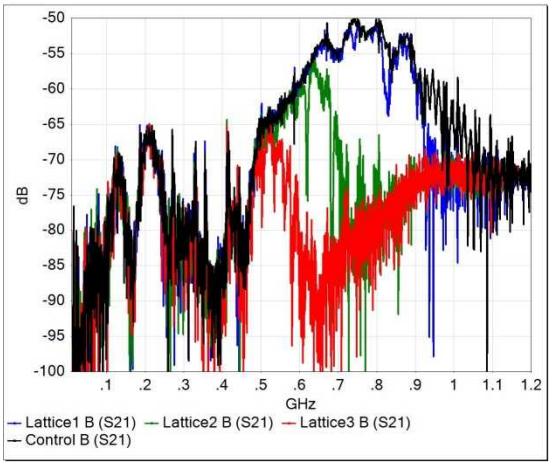

Figure 4. Frequency response for the B devices with 800 MHz transducers.

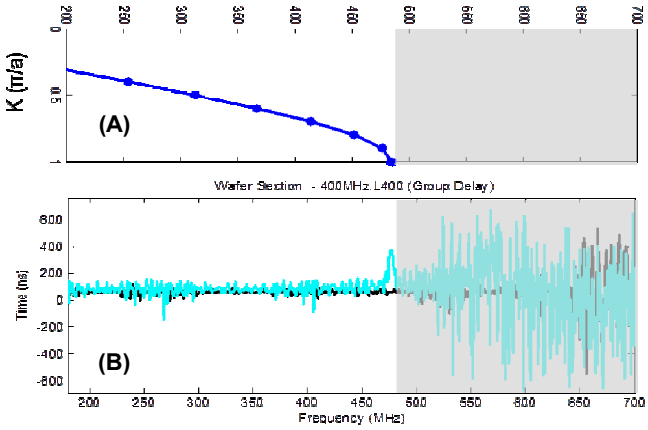

Figure 5. (A) Computed dispersion for S0 Lamb waves propagating in Lattice3. (B) Measured group delay for Lattice3 A.

(corresponding to a 600 micron spatial separation) is 62 ns for frequencies below the band-edge. However, for frequencies in the vicinity of the band edge the overall group delay increases to 370 ns. Since the phononic crystal region of this device is 400 microns in length, one can see that this excess group delay is consistent with a 8.5x reduction in group velocity due to the dispersion of this phononic crystal.

B. Time Domain Characterization

While the frequency response data above provide strong evidence of phononic impedance reduction, a more direct means of quantifying the phononic crystal effective impedance and the dispersive properties of phononic crystals is through time domain transmission and reflection measurements. Shown in Figure 6 and Figure 7 are the time domain transmission measurements for the Lattice A and B devices. At time t=0, a broad band pulse is launched from one of the transducers. For both the 400 and 800 MHz control devices, the pulse arrives at the opposite transducer, spaced 600 µm away, 62 ns later, corresponding to a S0 Lamb wave speed in the AlN plate of 9740 m/s. The narrow width of the received pulses for the control devices indicate that, as expected, the dispersion for the S0 Lamb wave is low in the thin AlN plate.

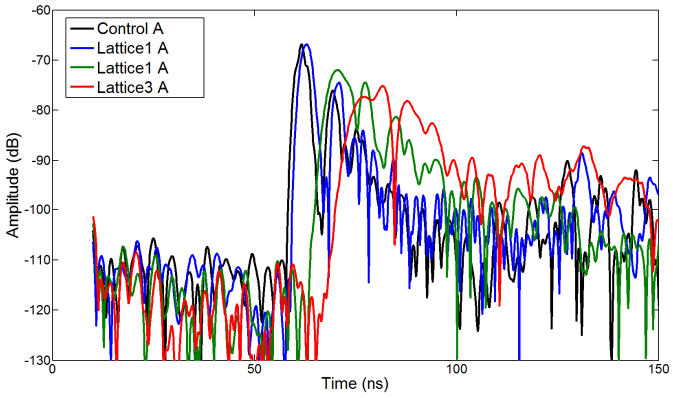

Figure 6. Measured transmission delay response to a broad band input pulse for the A devices with 400 MHz transducers.

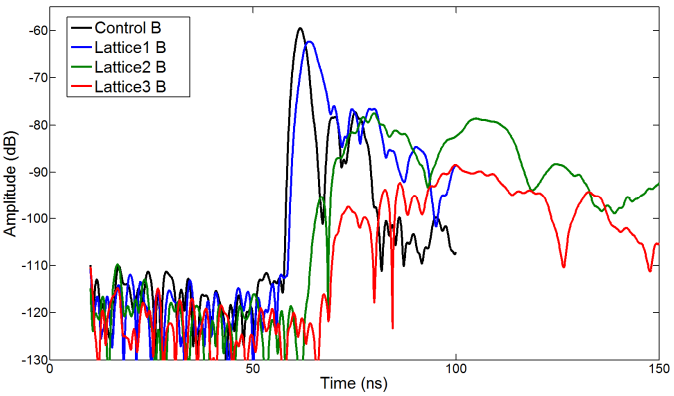

Figure 7. Measured transmission delay response to a broad band input pulse for the A devices with 400 MHz transducers.

As the phononic lattice is introduced, and the inclusion size is increased, the dispersion increases, as evidenced by an increase in the average measured delay given in Table 2 and the spreading out of the received pulses as the sound velocity changes dramatically over the transducer bandwidth. In the phononic crystal region the wave speed slows from 9740 m/s to an average of 5040 m/s for the Lattice3 devices with the largest inclusions.

V. Discussion

Within a bulk medium, phononic impedance is defined as $Z_o = \rho \cdot v$, where ρ is the material density, and v is the phase velocity of sound in the medium of interest. Within an effective medium, such as a phononic crystal, the complex dispersive properties result in a breakdown of this relationship. However, starting from a first principles consideration of impedance in periodic effective media, we have shown that the effective impedance of a phononic crystal medium is (to an excellent approximation) given by

$$Z_{eff} = \rho_{eff} \cdot v. \qquad (2)$$

Here, ρ_{eff} is the effective mass-density of the phononic crystal when averaging is performed over the unit cell of the periodic medium, and v_g is the group velocity of sound within the phononic crystal. According to Eq. 2, the average velocity reduction from 9740 m/s to 5040 m/s, coupled with the 39% effective mass density reduction from placing air holes in the AlN membrane to form a phononic crystal is consistent with an estimated 4.5x reduction in the effective impedance for the Lattice3 phononic crystals. In the vicinity of the band edge of the phononic crystal the effective impedance is further reduced by an estimated 22 times less than the bulk value, albeit over a narrow bandwidth.

VI. Conclusions

We have studied the dispersive properties of phononic crystals formed by etching air inclusions in thin, suspended plates of AlN. Even without realizing a full phononic bandgap significant dispersion for S0 Lamb waves was achieved and increased for larger inclusions. Wide band AlN S0 Lamb wave transducers at 400 MHz and 800 MHz were realized, allowing the phononic crystals to be characterized over a bandwidth of nearly 800 MHz using only these two transducer designs. An estimated 4.5x reduction in the effective phononic impedance is achieved over a broad bandwidth by placing a square lattice of 1.75 µm air holes on a 5 µm pitch in the suspended AlN plate. In the vicinity of the band edge, the estimated phononic impedance is reduced to 22 times less than the bulk value. In the future we plan to utilize these types of phononic crystals to improve the efficiency of optomechanical coupling over a broad bandwidth and to realize time domain signal processing circuits such as pulse compressors and correlators.

Acknowledgment

The authors would like to thank Dr. Ihab El-Kady and Dr. Ryan Camacho of Sandia National Laboratories for discussions on effective phononic media and phononic crystals. The authors would like to acknowledge the staff of the Microelectronics Develop Laboratory at Sandia National Laboratories for fabrication of the phononic crystal devices.

References

[1] R. H. Olsson III and I. El-Kady, *Meas. Sci. Tech*., vol. 20, 012002, 2009.

[2] S. Mohammadi, A. A. Eftekhar, A. Khelif, H. Moubchir, W. D. Hunt, and A. Adibi, "High Q micromechanical resonator in a two dimensional phononic crystal slabs," *Appl. Phys. Lett.*, vol. 95, 051906, 2009.

[3] N. Kuo, C. Zuo, G. Piazza, ""Microscale inverse acoustic band gap structure in aluminum nitride," *Applied Physics Letters*, Vol.95, Issue 9, 2009.

[4] M. Gorisse, S. Benchabane, G. Teissier, C. Billard, A. Reinhardt, V. Laude, E. Defay and M Aid, "Observation of band gaps in the gigahertz range and deaf bands in a hypersonic alunimum nitride phononic crystal slab," *Appl. Phys. Lett.*, vol. 98, 234103, 2011.

[5] T. T. Wu, L. C. Wu and Z. G. Huang, "Frequency band gap measurements of two-dimensional air/silicon phononic crystals using layered slanted finger interdigital transducers", *J. Appl. Phys*., vol. 97, pp. 094916-1-7 (2005).

[6] P. E. Hopkins, C. M. Reinke, M. F. Su, R. H. Olsson III, E. A. Shaner, Z. C. Leseman, J. R. Serrano, L. M. Phinney, I. El-Kady, "Reduction in the thermal conductivity of single crystalline silicon by phononic crystal patterning," *Nano Letters* 2011 11 (1), 107-112.

[7] H. Shin, W. Qiu, R. Jarecki, J. A. Cox, R. H. Olsson III, A. Starbuck, Z. Wang and P. T. Rakich, "Tailorable stimualted Brillouin scattering in nanoscale silicion waveguides," *Nature Communications,* **4**, 1944, 2013.

[8] M. Eichenfield, J. Chan, R. M. Camacho, K. J. Vahala and O. Painter, "Optomechanical crystals," *Nature,* 462, pp. 78-82, 2009.

[9] C. K. Campbell, "Applications of surface acoustic and shallow bulk acoustic wave devices," *Proc. of the IEEE,* vol. 77, no. 10, Oct. 1989.